KCI Concrete Journal
Vol. 13 No. 2 pp. 10-18, July 2001

NDT Determination of Cement Mortar Compressive Strength Using SASW Technique

Young-Sang Cho [1)]

[1)] Department of Architectural Engineering, Hanyang University, Korea

(Received February 13, 2001, Accepted July 2, 2001)

Abstract

The spectral analysis of surface waves (SASW) method, which is an in-situ seismic technique, has mainly been developed and used for many years to determine the stiffness profile of layered media (such as asphalt concrete and layered soils) in an infinite half-space. This paper presents a modified experimental technique for nondestructive evaluation of in-place cement mortar compressive strength in single-layer concrete slabs of rather a finite thickness through a correlation to surface wave velocity. This correlation can be used in the quality control of early age cement mortar structures and in evaluating the integrity of structural members where the infinite half space condition is not met. In the proposed SASW field test, the surface of the structural members is subjected to an impact, using a 12 mm steel ball, to generate surface wave energy at various frequencies. Two accelerometer receivers detect the energy transmitted through the medium. By digitizing the analog receiver outputs, and recording the signals for spectral analysis, surface wave velocities can be identified. Modifications to the SASW method includes the reduction of boundary reflections as adopted on the surface waves before the point where the reflected compression waves reach the receivers. In this study, the correlation between the surface wave velocity and the compressive strength of cement mortar is developed using one 36" x 36" x 4"(91.44x91.44x91.44 cm) cement mortar slab of 2,000 psi (140 kgf/cm^2) and two 36" x 36" x 4"(91.44x91.44x91.44 cm) cement mortar slabs of 3,000 psi (210 kgf/cm^2).

Keywords: test, nondestructive, cement, concrete, compressive strength, surface wave, spectral analysis.

1. Introduction

During the construction process and/or the lifecycle of concrete structures, the integrity of concrete needs to be inspected. A visual inspection provides information about cracks propagating to the surface of the material. To control quality of new constructions or to assess deterioration of existing slabs, destructive methods are usually used, in which sampling for laboratory tests is difficult and would appear in some cases more harmful than beneficial. Nondestructive tests are generally preferable. Some of nondestructive testing methods include ultrasonic based methods, resonant frequency method, magnetic/electrical methods, short-pulse radar methods, infrared thermographic techniques, acoustic emission methods, and stress wave methods. Some of these methods are currently used to determine structural properties and conditions.[(1)]

Stress wave methods, which are commonly used in reinforced concrete structures, include pulse-echo, impact-echo, impulse-response, and spectral analysis of surface wave (SASW) techniques. Although the SASW method was developed and used for the assessment of elastic properties of pavements and soil sites in geotechnical engineering,[(2, 3)] some researchers applied the technique to thin concrete slabs.[(4)] This method deals mainly with the estimation of phase velocity based on the spectral characteristics of the tested object.

In ideal conditions, SASW method requires presence of a thick layer of material so that the wave length is less than half of the thickness of the tested object approximately. Surface wave velocities can be evaluated using the interpretation methods developed by Bay and Stokoe.[(4)] In thin slabs, however, the reflected waves can arrive nearly simultaneously with surface waves to the receiving device. In this case, interpretation technique needs to be improved to eliminate the reflections from adjacent boundaries. This

study focuses on nondestructive assessment of single-layer concrete and mortar slabs using SASW method, which has the following advantages:

1. It requires measurements and access to only one side of the tested object.
2. When an impact is used to create a source wave, the majority of energy generated from the impact is imparted in the form of surface waves while the remainder goes into body waves.
3. The damping due to geometrical spreading for surface waves (cylindrical) is smaller than for body waves (spherical).
4. A stiffness profile (e.g. Young's modulus or shear modulus) can be obtained without knowing the layer thickness.

In this study, the theory of surface wave propagation, the current development of SASW method, experimental setup, interpretation procedure, reduction of boundary reflections, and evaluation of modified SASW technique are presented. Important elements in the SASW technique are the generation and detection of surface waves using a source and two receivers placed on the surface of testing object. A 2,000 psi (140 kgf/cm^2) and two 3,000 psi (210 kgf/cm^2) 36" x 36" x 4"(91.44x91.44x91.44 cm) cement mortar slabs are used in the experimental studies. The specimens are simply supported, and the boundaries at the bottom of slabs are free surfaces.

A 12 mm steel ball is used as a source dropped from a constant height. To reduce the boundary reflections, reflected waves are removed, and a bin low pass filter is used in the signal processing procedure. As one of the integrity analysis, the correlation between the early age concrete and mortar compressive strength and the surface wave velocity is studied using SASW method.

2. Development of SASW method

There are two kinds of surface waves: Rayleigh waves and Love waves. Rayleigh waves propagate along the surface of a uniform half space and decay exponentially with depth and diminish in amplitude with travel distance due to cylindrical spreading of energy. Love waves exist only if a low-velocity surface layer overlies a medium of higher velocity and are generated as the result of multiple reflections between the top and bottom of the low-velocity layer. This study concentrates on Rayleigh-type surface waves because 67 % of stress wave energy propagate is Rayleigh waves.

Layered systems have dispersive characteristics for Rayleigh waves. Rayleigh waves with different wavelengths will travel to different depths at different speeds. The depth to which a certain Rayleigh wave will propagate is approximately equal to its wavelength.[4] Rayleigh wave velocity is related to the material properties of the layer through which it propagates. The velocity of Rayleigh waves is a function of Poisson's ratio, and the nine tenths of the shear wave velocity approximately. The particle motion shows an elliptical motion as a result of longitudinal and transverse vibrations. Rayleigh waves are the main source waves in SASW method.

Heisey et al. in 1982[5] studied the feasibility of utilizing transient signals to construct dispersion curves (i.e., Fig. 1) using SASW method. Nazarian and Stokoe in 1984 and 1987[2, 3] developed the experimental and theoretical aspects of the SASW method as applied to geotechnical and pavement engineering field. Sanchez - Salinero et al. in 1987[6] studied analytically the most feasible source-receiver configuration. They indicated that a desirable distance between the source and the first receiver is equal to the distance between the adjacent receivers. Sheu et al. in 1987[7] recommended that, for the set-up suggested by Sanchez-Salinero et al. in 1987,[6] wavelengths greater than three times the distance between the receivers should not be considered. Gucunski and Woods in 1991[8] conducted an analytical study to quantify some of the problems associated with the alternative soft and hard layers. Bowen in 1992[9] evaluated cracked and repaired beams and columns using SASW method. Aouad in 1993[10] studied the relationship between the paving materials and temperature using SASW method.

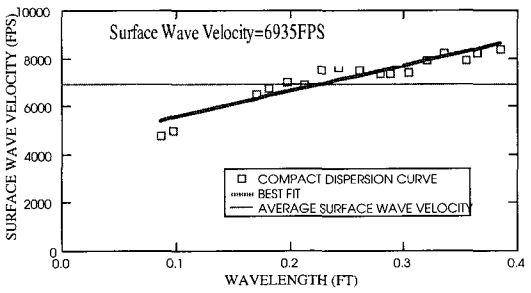

Fig. 1 Compact dispersion curve for 3 ksi mortar slab at the age of 16 days, with 3 inch receiver spacing

To make the SASW method practical, two simplifying assumptions have been made in the method.[3] First, it is assumed that a stack of horizontal layers can approximate the structure of a pavement and that the material properties of each layer are constant. Second, it is assumed that only plane Rayleigh waves are involved. The effect of body waves is ignored. The validity of this assumption has been evaluated by Sanchez-Salinero in 1987[6] in an analytical study and by Rix et al. in 1991[11] in an experimental study. The results from these studies show that the effect of ignoring body waves is quite justified as long as the source-receiver geometry relative to the wavelength is kept within certain limits. Stokoe and Kalinski in 1994 studied about

cracking on material damping(attenuation) measurements with surface wave was investigated. Material damping was evaluated using spectral ratios.

3. Experimental setup

Two 3,000 psi(210 kgf/cm^2) cement mortar slab specimens and one 2,000 psi(140 kgf/cm^2) cement mortar slab specimen were prepared. The size of each specimen is 36" x 36" x 4"(91.44x91.44x91.44 cm). Forms were stripped after two days and moved into lab environment. The specimens were cured with a temperature controlled at 75° F. Mix proportions for (cement: fine aggregate: water) are (1: 2.25: 0.5) by weight for the 3,000 psi(210 kgf/cm^2) slab, and (1: 3.25: 0.6) for the 2,000 psi(140 kgf/cm^2) slab. Type I Portland cement is used. Three different testing methods (SASW, resonant frequency, and cylinder test) are used to measure the mortar strength for comparison and verification purposes.

Instrumentation used in SASW method[9, 10] consists of an impact source, two receivers, and a recording device as shown in Fig. 2. The impact source should produce Rayleigh waves at a broad range of frequencies and at amplitudes higher than the background noise.[5, 8] The frequency range is a function of the contact time. Short contact time produces high frequencies that will propagate within the top portion of the specimen. Therefore, impact source should be selected considering the layer stiffness, the distance between two receivers, and the depth to be investigated. Investigation of object with finite thickness such as slabs requires use of impact sources that produce a short pulse with reasonable energy at high frequencies, i.e., frequencies up to 20 to 100 kHz.[12] Krstulovic-Opara, Woods, and Al-Shayea in 1996[13] used a rebound hammer as an impact source. However, they encountered problems of concrete surface deterioration caused by the repeated impacts and inability to reproduce consistent signals.

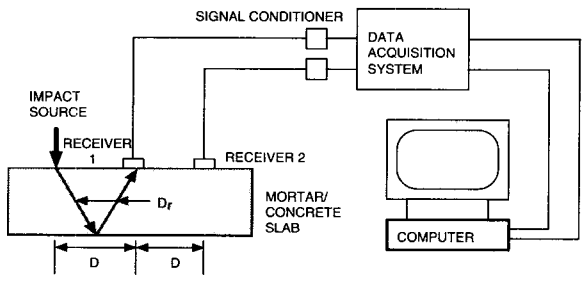

FIG. 2 Diagram of experimental set-up for SASW method

In this study, small steel balls and a ball peen hammer were initially tried. Small steel balls produced better results because steel balls, unlike ball peen hammers, can induce constant contact time, constant contact area, constant magnitude of impact, and high frequency signals. Therefore, only steel balls were used in the experiments. However, the drawback of using steel balls is that it is difficult to be applied to a vertical surface. Future research work should concentrate on developing an automatic signal generator that can control magnitudes, intervals, and directions of impact.

Two kinds of receivers were used in the SASW tests. The first was a PCB 352A78 accelerometer of which resonance frequency was greater than 45 kHz and calibration factor was 99.6 mv/g. The second one was a PCB 353B66 accelerometer of which resonance frequency was greater than 40 kHz and calibration factor was 100 mv/g. The PCB 352A78 accelerometer was used in most tests because of its wide frequency range compared to the PCB 353B66. In addition, the testing period with the same power supply is longer for PCB 352A78.

Good couplings between receivers and the slab surfaces are required. Greases were used in this experiment to couple the receivers on the slabs. The common receivers' midpoint (CRMP) geometry having the same distance, D, between two receivers and between the source and a receiver (as shown in Fig. 2) was used in this experiment. Based on the studies at several soil sites, Heisey in 1981[5] suggested that the distance between the two receivers should be less than two wavelengths and greater than one third of a wavelength.

The recording device is a two channel data acquisition system used for wave recording. Accelerometers are connected with signal conditioners before the recording device. The signal conditioners are required for powering accelerometers with built-in electronics. The signal conditioners offer system integrity meters, provide constant current power to accelerometers, and remove DC bias from sensor output signal.

In the resonant frequency test, an E-Meter manufactured by James Instruments Inc. was used to measure longitudinal fundamental resonant frequency.[14] The specification complies with ASTM C 215, Test Method for Fundamental Transverse, Longitudinal, and Torsional Frequencies of Concrete Specimens. Dynamic modulus of elasticity E_d = Dwn^2, where D = 0.01035 (L/bt), sec^2in^2, for a prism specimen, w = weight of specimen, lb, n = fundamental longitudinal resonant frequency, Hz, t,b = dimensions of cross section of prism, in, and L = length of prism, in. Young's modulus is estimated at 67 % of dynamic modulus of elasticity.[15] A 4" x 4" x 12"(10.16x10.16x30.48 cm) of 3,000 psi(210 kgf/cm^2) prism and a 4" x 4" x 12" (10.16x10.16x30.48 cm) of 2,000 psi(140 kgf/cm^2) prism were prepared from the same batch of cement mortar for the slabs. In the cylinder test, mortar cylinders of 0.076 m (3 in.) diameter and 0.15 m (6 in.) height were compressed

for the measurement of the compressive strength. The cylinders were made from the same batch and stored next to the cement mortar slabs.

4. Signal processing procedure

When SASW measurements are performed, a source and two receivers are placed on the cement mortar slabs such that the distance from the source to the first receiver is equal to the distance between the two receivers as shown in Fig. 2 Several transient pulses generated by dropping steel balls are recorded in a data acquisition system. The data acquisition system is used to capture the receiver outputs denoted by x(t) and y(t) for receivers 1 and 2 respectively. Then x(t) and y(t) are transformed to the frequency domain X(f) and Y(f) through a fast Fourier transform.[16] The cross power spectrum G_{XY} between the two receivers is defined as X(f)*Y(f), where X(f)* denotes the complex conjugate of X(f). The experiment and the procedure are repeated 16 times to obtain the averaged final cross power spectrum. The phase shift $\theta_{xy}(f)$, which represents physically the number of cycles that each frequency possesses in distance D between the two receivers, can be computed as

$$\theta_{XY}(f) = \theta_X(f) - \theta_Y(f) = \tan^{-1}[\mathrm{Im}(G_{XY})/\mathrm{Re}(G_{XY})] \quad (1)$$

where

$\theta_{XY}(f)$ = phase shift of the cross power spectrum in degrees at each frequency,

$\mathrm{Im}(G_{XY})$ = imaginary part of the cross power spectrum at each frequency,

$\mathrm{Re}(G_{XY})$ = real part of the cross power spectrum at each frequency,

f = frequency.

To clarify the process, typical phase information from cross power spectra is shown in Fig. 3 (d) and Fig. 4 (d) for the 3000 psi(210 kgf/cm^2) mortar slab at the age of 16 days with 3-inch receiver spacing. The phase plots shown in Fig. 3 (d) and Fig. 4 (d) oscillate between -180 and 180 degrees. These are the standard method of demonstrating the phase. The step to find the actual phase of a frequency is to count the number of full 360-degree cycles preceding the frequency and to add that to the fraction of the last cycle of the frequency. This process is called unfolding of the phase.[3] The sign of the phase has to be changed because the recovered phase always bears a negative sign. However, the negative sign is omitted for convenience.[7] From the cross power and the coherence magnitude, the frequency components with low quality should be removed to circumvent a misinterpretation of phase information. This operation is called masking.

By using the principle of a rotating vector, a phase shift of 360 degrees is equivalent to the travel time of one period For a harmonic wave, the period, T, is the reciprocal of the frequency of that wave (i.e., T = 1/f). Therefore, the travel time, t(f), from receiver 1 to receiver 2 can be computed by

$$t(f) = \theta_{XY}(f) \cdot T / 360^\circ = \theta_{XY}(f) / (360^\circ \cdot f) \quad (2)$$

The surface wave velocity, $V_R(f)$, and the wavelength, $\lambda_R(f)$, can then be determined by

$$V_R(f) = D / t(f) \quad (3)$$

$$\lambda(f) = V_R(f) / f \quad (4)$$

where t(f) = time delay(travel time) between two receivers as a function of frequency, and D = distance between the two receivers.

The plot of surface wave velocity $V_R(f)$ versus wavelength λ (f) is called a dispersion curve.[11] The data points of experimental dispersion curve are usually compressed into a smaller number of data points by averaging a certain number of experimental data points into one data point. The dispersion curve after being compressed is called a compact dispersion curve.

In addition, values of coherence functions are calculated in these measurements. The coherence function is the ratio of the output power caused by the measured input to the total measured output. If the system is ideal (noise free), the coherence will be unity for all frequencies. If some noise is generated in the system, the coherence is less than unity since the total measured output includes not only the output power due to the measured input but also noise output due to the input noise and noise at the output side. The coherence function, $\gamma^2(f)$, is mathematically defined as

$$\gamma^2(f) = |G_{XY}|^2 / (G_{XX} \cdot G_{YY}) \quad (5)$$

where

$|G_{XY}|$ = magnitude of the cross power spectrum,

$G_{XX} = X(f)^* \cdot X(f)$ = power spectrum of receiver 1, and

$G_{YY} = Y(f)^* \cdot Y(f)$ = power spectrum of receiver 2.

The quantities of the magnitude of the cross power spectrum and power spectra are arithmetically averaged in the frequency domain over multiple input record.[16]

The magnitude of the cross power spectrum and power spectrum also has the following relationship [17]:

$$|G_{XY}|^2 \le G_{XX} \bullet G_{XY} \quad (6)$$

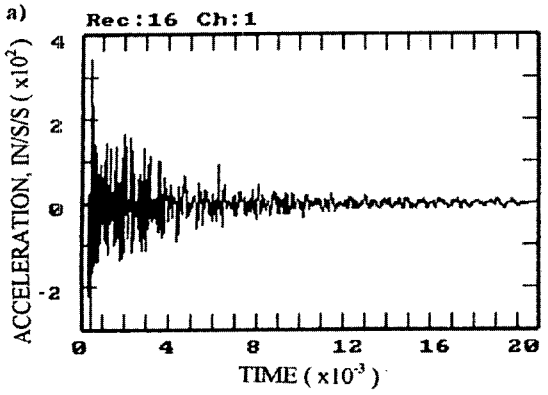

(a) Time domain signal at receiver 1

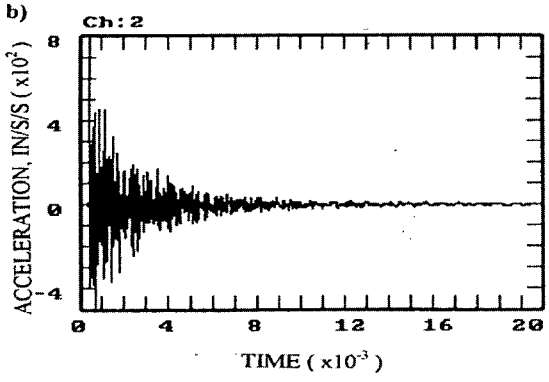

(b) Time domain signal at receiver 2

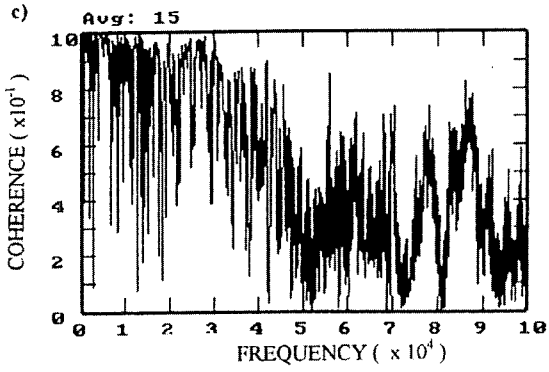

(c) Coherence function

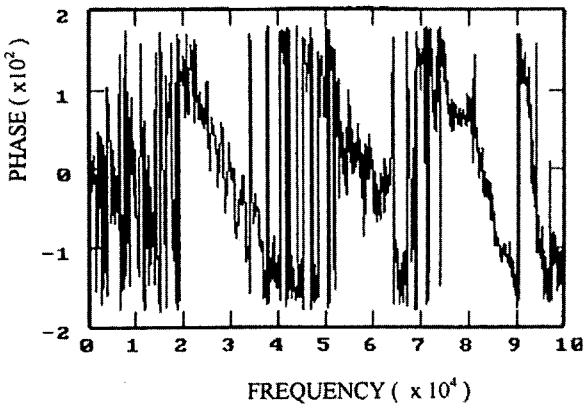

(d) Cross power spectrum

Fig. 3 Signals before removing reflections

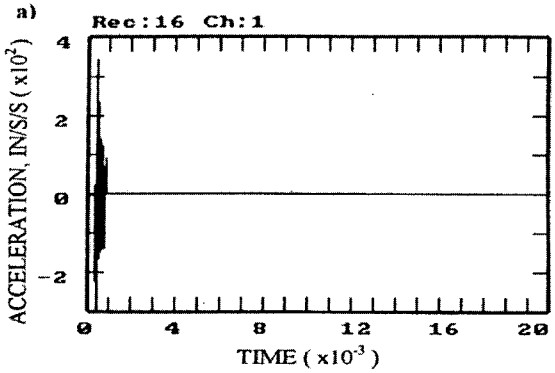

(a) Time domain signal at receiver 1

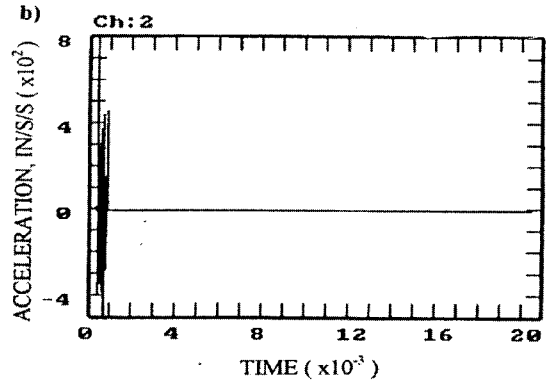

(b) Time domain signal at receiver 2

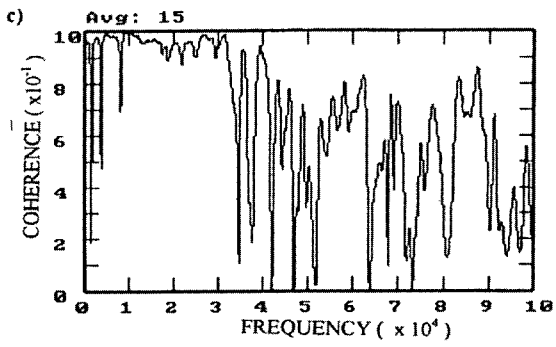

(c) Coherence function

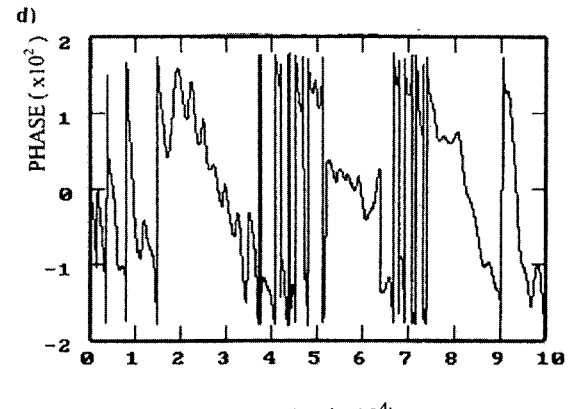

(d) Cross power spectrum

Fig. 4 Signals after removing reflections

The quantities of the magnitude of the cross power spectrum and power spectra are arithmetically averaged in the frequency domain over multiple input record.[16] The magnitude of the cross power spectrum and power spectrum also has the following relationship[17]

$$| G_{xy} |^2 \leq G_{xx} \bullet G_{xy} \quad (6)$$

The coherence function is related to the signal-to-noise ratio by[2] :

$$(S/N) = \gamma^2(f) / [1 - \gamma^2(f)] \quad (7)$$

The coherence function is a good tool for assessing the quality of the observed signals. The coherence function has values between zero and one in the range of frequencies being measured. A value of one indicates perfect correlation between signals being picked up by the receivers which is equivalent to a signal-to-noise ratio of infinity. A value of zero for the coherence function at a frequency represents no relation between the signals being detected.

The phase data with low coherence value are discarded before the dispersion curve is constructed. However, a low coherence may not necessarily suggest bad correlation between the signals. Some reasons for low coherence besides the presence of noise are nonlinearity of the system, and multiple input signals, resolution bias errors in the spectral estimates in the system, etc. A typical coherence function is shown in Fig. 4 c) for the 3,000 psi(210 kgf/cm^2) mortar slab at the age of 16 days with 3-inch receiver spacing.

5. Reduction of boundary reflections

To improve the quality of signal condition, windowing functions[18] are applied to the time domain signals before the spectral analysis is performed. Windows are necessary to obtain better phase diagrams and affect the smoothness and magnitude of the spectrum. These windowing functions consist of some classical filtering functions such as Hanning, Hamming, flat top, etc. They have different spectral characteristics. Some will minimize the picket fence effects or spectral leakage. Some will have different effects on the accuracy of either amplitude or frequency.[18] They are basically weighting functions in time domain. There are also filtering and editing type of windowing functions such as bin low pass, bin high pass, bin band pass, bin band stop, and exponential. These can be considered as extended functions of rectangle window (i.e., unit box-car window).

The purpose of these windowing functions is to edit out systematically the unwanted part in the recorded signal. For example, bin low pass filter can edit out echoes after the first strong echo while bin band pass filter can preserve the second echo. If source impacts distort the spectrum, then the exponential filter can be used to de-emphasize the distortion. A proper filtering function can be selected based on the signal of interest. All data in the pass band is preserved by a 1 multiplier, and all data outside the pass band is discarded by a 0 multiplier. Any discontinuity in time domain signals must be avoided for proper filtering process. These windowing functions can be viewed as a tool to eliminate the noises (transducer drifts) after impact sources are applied so that the spectra will not be distorted.

Bay and Stokoe in 1990[4] encountered reflection problems from adjacent boundaries. They solved the problems by using windowing function that eliminates most of the reflection-induced noise. However, use of a windowing function can also be detrimental by possibly smearing detail in the frequency domain.[4] Krstulovic - Opara, Woods and Al - Shayea in 1996 had the same reflection problems in testing a concrete wall. They didn't use the windowing function process, but they recommended testing its applicability for a future research work. In this study, a new approach is developed to eliminate the reflection problem.

The new approach to reduce boundary reflections adopts only the waves before the point where the reflected compression waves reach the near receiver from the source. This can be done because reflection waves arrive after the arrival of surface waves. Reflected waves cause inaccurate Rayleigh wave (surface waves) profiles. To find the point where compression waves arrive at the near receiver, the following formula can be used :

$$T = D_r / V_p = N t \quad (8)$$

where T and Dr are the time and distance for reflected compression waves to travel from the source to the near receiver, Vp is the velocity of the compression wave, Δt is the sampling rate, and N is the number of sampling points before the reflected compression waves reach the near receiver.

As D_r, V_p, and Δt are known, the number of sampling point N after which waves will be eliminated can be obtained. Fig. 3 a), b) show the signals recorded at receiver 1 and receiver 2 with 3 inch spacing, respectively, for the case of 3000 psi and 16 days' age before reflection waves are removed. Fig. 3 c) shows the coherence function of the two signals, and Fig. 3 d) shows the cross power spectrum. As shown in the figures of the coherence function and the cross power spectrum, significant reflections and noises exist. Fig. 4 a), b) show the same signals after reflections are removed. Fig. 4 c), d) shows the corresponding coherence function and cross power spectrum. It can be seen that the coherence function and the cross power spectrum are

clean and legible. This will contribute to the generation of more accurate dispersion curves.

6. Evaluation of modified SASW technique

In this experimental study, each specimen was tested at 9 positions, evenly spaced and 6 minimum away from the boundaries of the slab. Each position in the same specimen having the same compressive strength should produce a similar result. Measurements were conducted on the 3rd, 6th, 10th, 16th, 20th, and 31st day after pouring the cement mortar. Each test collected 16 signal samples for averaging. Some representative cross power spectra and coherence functions for the 3,000 psi(210 kgf/cm^2) and the 2,000 psi(140 kgf/cm^2) specimens, respectively, were used for the construction of dispersion curves.

To obtain these cross power spectra and coherence functions, the recorded signals were first processed to remove reflections from the adjacent boundaries. These signals were then transformed from time domain to frequency domain using fast Fourier transform. After taking averages of 16 signals, they were further processed to obtain the cross power spectra and coherence functions. These cross power spectra show reasonable phase differences so that the corresponding dispersion curves can be plotted.

The compact dispersion curves for the 3,000 psi(210 kgf/cm^2) specimens (Fig. 1) and for the 2,000 psi(140 kgf/cm^2) specimen were obtained after a masking process which eliminates unnecessary portions of the cross power spectra. These compact dispersion curves are the representative data measured at different mortar ages. The figures show data points, the best-fit curve, and the average surface wave velocity. The dispersion curves show the trend of a horizontal line except some differences in surface wave velocity which may have been caused by a differential curing due to air dry after the mortar pouring date. These surface wave velocities are used to correlate with compressive mortar strengths. Fig. 5 (a) and Fig. 6 (a) show a gradual increase in surface wave velocity from the 3rd day to the 31st day after the pouring of cement mortar. The increase in surface wave velocity reasonably agrees with the increase in the mortar strength obtained from the resonant frequency and the cylinder test methods as shown in Fig. 5 (b) and Fig 6 (b). Fig. 7 and Fig. 8 show the correlation between the

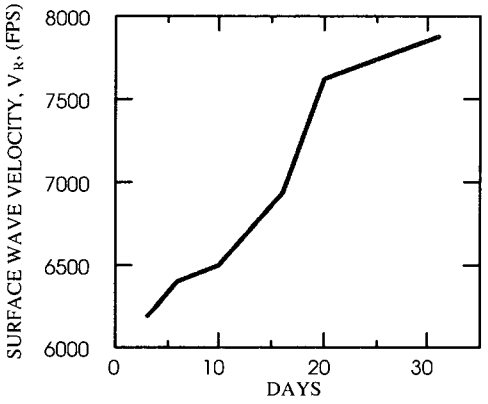

(a)

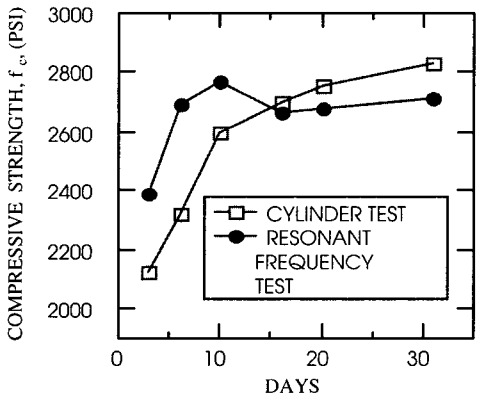

(b)

Fig. 5 Surface wave velocity and compressive strength at different ages of the 210 kgf/cm^2 specimens

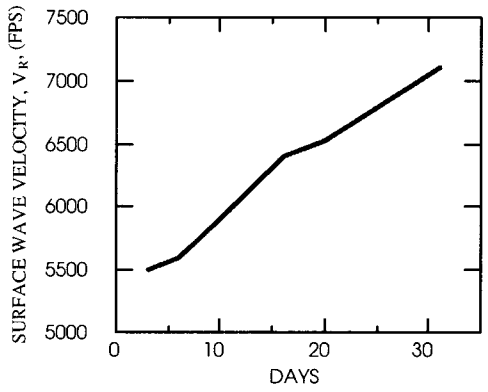

(a)

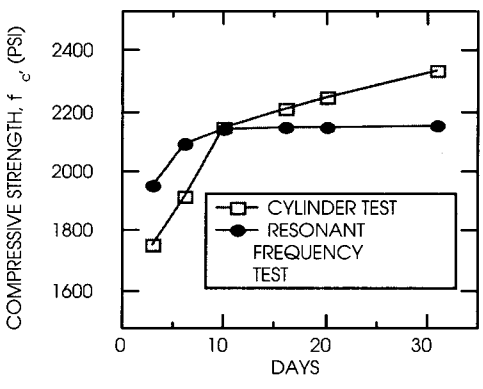

(b)

Fig. 6 Surface wave velocity and compressive strength at different ages of the 140 kgf/cm^2 specimens

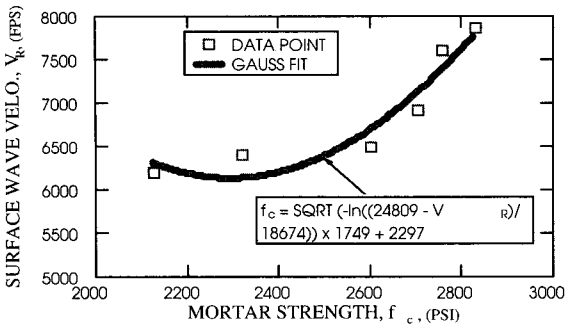

Fig. 7 Correlation between surface wave velocity and mortar strength of the 210 kgf/cm^2 specimens from ages of 3 days to 31 days

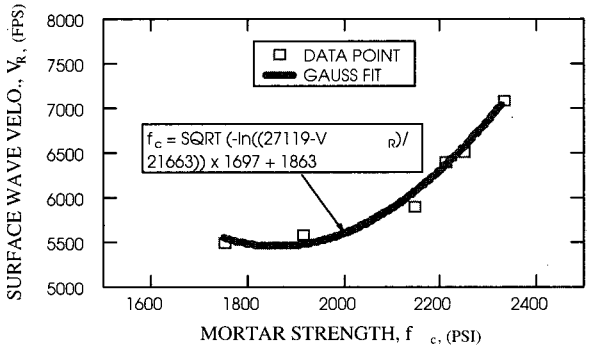

Fig. 8 Correlation between surface wave velocity and mortar strength of the 140 kgf/cm^2 specimens from ages of 3 days to 31 days

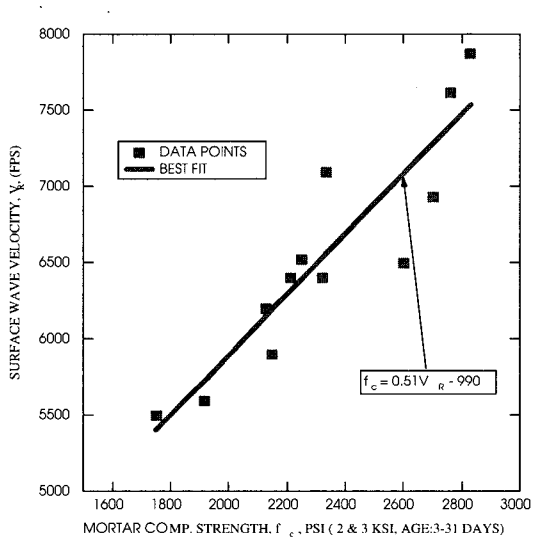

Fig. 9 Correlation between surface wave velocity and mortar compressive strength for the 140 kgf/cm^2 and 210 kgf/cm^2 specimens from ages of 3 days to 31 days

surface wave velocity and the compressive strength of the 2,000 psi(140 kgf/cm^2) and 3,000 psi(210 kgf/cm^2) cement mortar slabs, respectively. Fig. 9 shows the combined correlation between the surface wave velocity and the mortar compressive strength after combining the test results of 2,000 psi(140 kgf/cm^2) and 3,000 psi(210 kgf/cm^2) cement mortar slabs. Based on the test results, the cement mortar strength can be found from the following best fit equation :

$$f_C = 0.51V_R - 990 \quad (9)$$

where fc is the mortar compressive strength in psi and V_R is the surface wave velocity in fps.

7. Conclusions

Based on the experiments and discussions, conclusions have been made as follows.

1). In the experiment of finite thickness cement mortar slabs, the reflections from boundaries have been reduced by adopting only the waves before the point where the reflected compression waves reach the receivers from the source.

2). It appears that the correlation between the surface wave velocity and the cement mortar strength in finite thickness mortar slabs has been successfully developed in the current experimental study, even though the SASW method was originally developed only for an infinite half space with multi-layer media. The correlation has been made between surface wave velocities which was obtained form the compact dispersion curves of different specimens and the cement mortar compressive strengths obtained from different cement mortar cylinders.

3). The test results can be used in the quality control and the integrity analysis of concrete slab construction.

Acknowledgements

The support by the advanced Structural RESearch Station (STRESS) at Hanyang University on this study is gratefully Acknowledged.

References

1. Malhotra, V. M., and Carino, N. J., "CRC Handbook on Nondestructive Testing of Concrete," CRC Press, Inc., Boca Raton, Florida, 1991.
2. Nazarian, S., "In Situ Determination of Elastic Moduli of soil Deposits and Pavement systems by Spectral-Analysis-of-Surface-Waves Method," PhD Thesis, Department of Civil Engineering, The University of Texas at Austin, 1984.
3. Nazarian, S., Yuan, D., and Baker, M. R., "Rapid Determination of Pavement Moduli with Spectral-Analysis-of-Surface-Wave Method," Transportation Research Report, 1243-1, The Center for Geotechnical and High Way Materials Research, The University of Texas at El Paso, 1995.
4. Bay, J. A., and Stokoe, II, K. H., "Field Determination of

Stiffness and Integrity of PCC Members Using the SASW Method," Proceedings of Nondestructive Evaluation of Civil Structures and Materials Conference, University of Colorado at Boulder, 1990, pp.71- 86.

5. Heisey, J.S., Stoke, K. H., II, and Meyer, A. H., "Moduli of Pavement Systems from Spectral Analysis of Surface Waves," Transportation research record, No. 852, Washington, D.C., 1982, pp. 22-31.
6. Sanchez-Salinero, I., "Analitical Investigation of Seismic Methods Used for Engineering Applications," Ph.D. Thesis, the University of Texas at Austin, 1987.
7. Sheu, J. C., "Application and Limitations of the Spectral-Analysis-of-Surface-Waves Method," Ph.D. Thesis, Department of Civil Engineering, The University of Texas at Austin, 1987.
8. Gucunski, M., "Generation of Low Frequency Rayleigh Waves for the Spectral-Analysis-of-Surface-Waves Method," PhD Thesis, Department of Civil and Environmental Engineering, University of Michigan, Ann Arbor, 1991.
9. Bowen, B. R., And Stoke II, K. H., "Evaluation of Cracked and Repaired Beams and Columns Using Surface Stress Waves," Proceedings of the Tenth World Conference on Earthquake Engineering, Madrid, Spain, 1992.
10. Aouad, M. F., "Evaluation of Flexible Pavements and Subgrades using the Spectral-Analysis-of-Surface-Waves (SASW) Method," Ph.D. Thesis, the University of Texas at Austin, 1993, pp. 15.
11. Rix, G. J., "Experimental Study of Factors Affecting the Spectral-Analysis-of-Surface-Waves Method," Ph.D. Thesis, Department of Civil Engineering, The University of Texas at Austin, 1988.
12. Cho, Y. S., and Lin, F. B., "Nondestructive Determination of In-Place Concrete Strength Using Spectral Analysis of Surface Waves," Proceedings of Nondestructive Evaluation of Civil Structures and Materials Conference, University of Colorado at Boulder, 1996, pp. 381-393.
13. Krstulovic-Opara, N., Woods, R. D., and Al-Shayea, N., "Nondestructive Testing of Concrete Structures Using the Rayleigh Wave Dispersion Method," ACI Materials Journal, Vol. 93, No. 1, Jan., 1996, pp. 75-86.
14. Whitmoyer, S. L., and Kim, Y. R., "Determining Asphalt Concrete Properties via the Impact Resonant Methods," Journal of Testing and Evaluation, JTEVA, Vol. 22, No. 2, March 1994, pp. 139-148.
15. Mindess, S., and Young, J. F., "Testing Hardened Concrete Nondestructive Method," 1981.
16. Hitunen, D. R., "Experimental Evaluation of Variables Affecting the Testing of Pavements by The Spectral-Analysis-of-Surface-Waves Method," Ph.D. Thesis, Department of Civil Engineering, University of Michigan, Ann Arbor, 1988.
17. Bendit, J. S., and Piersol, A. G., "Measurement and Analysis of Random Data," John Wiley & Sons, Inc., New York, 1966.
18. Proakis, J.G., and Manolakis, D. G., "Digital Signal Processing," 3rd Ed., Prentice Hall, Upper Saddle River, NJ 07458, 1996, pp. 448-493.